

In situ x-ray-scattering study of the Au(001) reconstruction in alkaline and acidic electrolytes

I. M. Tidswell, N. M. Marković,* C. A. Lucas, and P. N. Ross

Materials Sciences Division, Lawrence Berkeley Laboratory, One Cyclotron Road, Berkeley, California 94720

(Received 24 August 1992; revised manuscript received 27 January 1993)

X-ray scattering from the solid/liquid interface of a Au(001) single crystal in 0.1 M potassium hydroxide and 0.1 M perchloric acid electrolytes has been measured. In both solutions the Au surface reconstruction consists of an incommensurate-hexagonal monolayer with a structure similar to the clean annealed vacuum surface at room temperature. In KOH electrolyte the reconstruction is aligned along the [110] direction, unlike the vacuum and perchloric acid interfaces, where the reconstruction is rotated $\pm(0.5-0.8)^\circ$ from the [110] direction. In KOH solution the reconstruction forms rapidly at electrode potentials below -0.25 V (versus the saturated calomel electrode) and is lifted in a narrow potential region (40 mV) above -0.10 V, very close to the estimated potential of zero charge (PZC) for the reconstructed surface. In perchloric acid solution the reconstruction forms much more slowly at potentials just below the PZC of the unreconstructed surface, and is stable up to approximately 0.30 V, which is just positive of the PZC. In KOH solution the stability of the reconstruction is controlled primarily by the interaction of the surface with hydroxyl anions. The controlling mechanism in perchloric acid is unclear.

I. INTRODUCTION

Although the surface reconstruction of the 5d fcc metals (Au, Pt, and Ir) in vacuum was discovered 25 years ago,¹ only recently have the interface structures of these metals with liquids been studied *in situ*. This long delay arose due to the paucity of probes for studying "buried interfaces," with most traditional ultrahigh vacuum (UHV) studies using electron probes, such as low-energy electron diffraction (LEED), to elucidate surface structures. LEED patterns from the room-temperature annealed Au(001) surface revealed a " (5×20) " structure, indicative of a hexagonal overlayer on the square bulk lattice.² Initial speculation about the possible reconstruction of the Au(001) surface in contact with an electrolyte arose from changes to the pseudocapacitance after the crystal had been held at a potential just above that at which hydrogen is evolved.³

The earliest attempts at direct determination of the surface structure of gold immersed in an electrolyte used *ex situ* LEED.^{4,5} For these studies the surface was prepared using standard UHV techniques (sputtering and annealing), after which the crystals were transferred through an inert gas to the electrochemical cell. The crystals were then removed from the electrolyte under potential control and transferred back into the vacuum chamber where LEED analysis was conducted. Despite this somewhat cumbersome approach, these studies revealed that the Au(001) surface remained reconstructed when removed from HClO₄ solution provided the potential was kept below 0.45 V [versus the saturated calomel electrode, SCE (Ref. 6)]. After removing the crystal from the electrolyte at higher potentials, however, only the unreconstructed (1×1) structure was observed. Although techniques such as pseudocapacitance, reflectance spectroscopy, and second-harmonic

generation have since been used to study the kinetics of these systems, they are not capable of direct determination of surface structure. For reviews of these techniques, see Ref. 7. More recently, the utilization of scanning tunneling microscopy^{8,9} (STM) and x-ray surface scattering^{10,11} have allowed microscopic *in situ* studies of surface reconstruction and specific adsorption of cations. These studies^{9,11} have revealed that the surfaces of Au(001) single crystals in HClO₄ solution are indeed reconstructed in the absence of specifically adsorbed ions or at sufficiently positive potentials.

The most useful techniques for UHV surface reconstruction determination of the Au(001) surface to date have been LEED,² STM,¹² and x-ray surface diffraction and reflectivity.^{13,14} The structures derived from these studies, while yielding slightly different information in each case, are in excellent agreement. They indicate that the surface reconstruction consists of a single buckled slightly distorted hexagonal overlayer aligned close to the [110] bulk direction. X-ray-diffraction measurements can give detailed structural information in both the surface normal¹³ and in-plane directions.¹⁴ Measurements of the Au(001) specular crystal truncation rod¹³ (CTR) have found that at room temperature the best one-layer fit to the specular reflectivity indicates that the top layer is expanded away from the expected bulk position by 20% of a bulk lattice spacing. The top layer density is 1.25 times that of a bulk layer and the rms surface normal displacement is enhanced (0.3 Å). Grazing-incidence x-ray studies¹⁴ have shown that the room-temperature surface reconstruction consists of an incommensurate slightly distorted hexagonal overlayer. The overlayer is aligned approximately with the [110] direction, although the detailed in-plane surface structure is somewhat dependent on the rate of cooling of the surface. For slowly cooled samples, the hexagonal overlayer is almost exclusively rotated approximately $\pm 0.8^\circ$ from

the [110] direction, with a very small fraction of the domains unrotated. The peaks are centered at the (1.206 1.206) in-plane position [indexed to the bulk gold Bragg peaks at (220) in the plane].

Theoretical studies of the Au(001) vacuum interface^{15,16} suggest that the reconstruction forms because the energy gained from the formation of the more compact reconstructed top layer is greater than the energy lost due to the loss of registry with the substrate. The energy difference between the relaxed (1 × 1) surface and the reconstructed surface is calculated^{15,16} to be of order 0.1 eV/atom. At room temperature, however, spontaneous conversion of the (1 × 1) surface to the reconstructed "(5 × 20)" surface is inhibited by the energy barrier for surface self-diffusion, and annealing the crystal above approximately 370 K is necessary for formation of the reconstruction.⁷

In situ STM measurements of the Au(001) surface in 0.1 M HClO₄ by Gao, Hamelin, and Weaver⁹ found that the surface was reconstructed for potentials⁶ less than approximately -0.35 V, forming corrugated quasihexagonal domains with two slightly different but distinct structures. Holding the potential at approximately 0.10 V lifted the reconstruction in approximately 10 min. The reconstruction reformed in a few minutes on holding the potential at -0.4 V. X-ray reflection and diffraction studies by Ocko *et al.*¹¹ found that the surface reconstruction began lifting at about⁶ 0.2 V (on scanning the potential at 0.2 mV/sec), and reformed when the potential was reduced below approximately -0.2 V. Specular CTR scans showed that the structure of the reconstructed surface was very similar to the UHV surface described above, except that the rms surface displacement of the top layer was somewhat greater. The reconstruction peak was initially aligned along the [110] direction but after potential cycling was rotated ±0.8° away from this direction. Again the reconstruction took several minutes to reform.

In contrast to the many studies of the Au(001) surface in the presence of acid and neutral electrolytes, the Au(001)/alkaline electrolyte interface has been studied relatively little. Hamelin *et al.*¹⁷ reported cyclic current-potential curves (so-called "cyclic voltammograms" or CV's) of an Au(001) crystal in 0.11 M NaOH electrolyte which featured a small peak at approximately⁶ 0.0 V which they speculated was due to the lifting of the reconstruction. The reduction of oxygen in alkaline electrolytes for Au(001) was also studied using the rotating disk electrode technique.^{18,19} To our knowledge, however, no direct studies of the structure of the Au(001) interface in alkaline electrolytes have been conducted.

In this paper we report an x-ray scattering study of the Au(001) surface in 0.1 M solutions of HClO₄ and KOH. Our results in HClO₄ solution are very similar to those obtained by Ocko *et al.*¹¹ The reconstructed surface in KOH solution, however, has a somewhat different structure and forms more rapidly. X-ray scattering techniques are well suited for this type of study because of the nondestructive nature of the probe and the relatively long penetration lengths which permit *in situ* crystal/electrolyte studies. Several recent review papers which describe x-ray scattering in some detail are available.²⁰

II. EXPERIMENT

A. Sample preparation and characterization

The gold single crystal used in these studies was spark cut to approximately 0.5° of the (001) crystal face, annealed at 1070 K for 150 h, and mechanically polished. The final crystal was approximately 8 mm in diameter and 4 mm thick with a surface area of 62 ± 5 mm². After polishing and placing the crystal in an UHV system, no LEED diffraction spots were observed, suggesting a damaged surface. The damaged layer was removed by simultaneously heating the sample to approximately 950 K and sputtering in the presence of Ar for about 20 hours. After this treatment, and a further anneal to approximately 600 K, LEED revealed the familiar (5 × 20) reconstruction pattern.

Immediately prior to placing the sample in the electrochemical cell, a final "flame annealing" surface preparation was carried out. This process, which was very similar to that used for the preparation of platinum single crystals by Marković *et al.*,²¹ consisted of annealing the crystal in a hydrogen flame for approximately two minutes, such that the crystal had a dull red glow with the room lights dimmed, then placing the crystal in a flowing stream of hydrogen until it had cooled to approximately 370–420 K. After removal of the crystal from hydrogen a drop of water was placed on the crystal to protect the surface during subsequent manipulation. During this procedure, the crystal was exposed to air for only 5–10 sec.

The quality of the flame annealed surface was characterized by vacuum and electrochemical techniques. After transfer to the UHV chamber, LEED analysis revealed a (1 × 1) surface with sharp, bright diffraction spots. A short cycle of sputtering and annealing (approximately 2 min for each) resulted in recovery of the (5 × 20) pattern. A previous study found that the flame annealed surface cooled in gas was reconstructed. Placing a drop of water on the surface did not lift the reconstruction, although cooling the crystal predominately in water did result in a (1 × 1) surface.²² In our x-ray experiment the reconstruction was formed using electrochemical means.

A second electrochemical characterization was carried out both before and after the gold crystal was placed in the x-ray cell. This was performed using the hanging meniscus technique,²¹ in which the crystal is dipped into the electrolyte and then slowly removed such that only the crystal face of interest makes contact with the electrolyte. A gold counter electrode and palladium reference electrode previously charged with hydrogen were used. While any individual Pd reference electrode was found to be stable for periods of days, some variability was found between the reference electrodes after charging the Pd with hydrogen. We estimate that the uncertainty in the quoted potential is approximately ±50 mV. The potentials were converted from the Pd/hydrogen reference to the SCE reference scale used in this paper by the subtraction of 250 and 970 mV for 0.1 M HClO₄ and KOH solutions, respectively. The electrolyte solutions

were prepared by dissolving concentrated HClO_4 (J. T. Baker, Ultrex) and KOH pellets (J. T. Baker Reagent) into pyrolytically-triply-distilled water to form 0.1 M solutions. The electrolytes were deaerated prior to electrochemical cycling. The sample potential was controlled using a BAS CV27 potentiostat.

B. X-ray measurement

X-ray scattering measurements were performed on Beamline X16B at the National Synchrotron Light Source. This beamline consists of a vertical-focusing mirror and a single horizontal bent asymmetric $\text{Ge}(111)$ crystal monochromator set to pass x rays of wavelength 1.691 Å.

X-ray measurements were taken using the cell shown in Fig. 1. The body of the cell was machined from Kel-F (DuPont) and all fittings and tubes used were teflon. The sample was held in a Kel-F collet which was easily mounted into both the hanging meniscus holder and the x-ray cell. During the course of the x-ray measurements, electrolyte leaked around the crystal, making contact with all surfaces. This resulted in CV's contaminated with current flowing through unpolished and unaligned surfaces. All prominent features of the hanging meniscus CV were, however, observed in CV's measured in the x-ray cell. These tests were performed with the polypropylene film inflated. Prior to the x-ray experiments the polypropylene film was retracted to cover the surface. We estimate the surface electrolyte film in this configuration to have a thickness of 10–50 μm . Electrolyte was introduced into the cell using a glass syringe connected via teflon tubing. Once the film was drawn over the crystal it remained in place, typically for periods of a day or so while x-ray measurements were taken. For the duration of the x-ray experiment the cell was positioned in an outer cell which was flushed with ultra-pure nitrogen to prevent oxygen from diffusing through the polypropylene x-ray window.

III. X-RAY SCATTERING FROM SURFACES

Measurement of the specular CTR was used to study the structure of the surface in the surface normal direc-

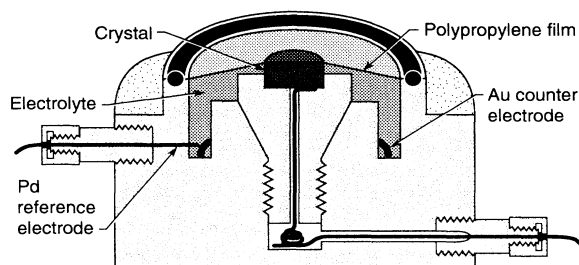


FIG. 1. A sectional view of the electrochemical x-ray scattering cell. Not shown are two electrolyte and one counter-electrode feedthroughs.

tion. Figure 2 shows a representation in reciprocal space of the scattering from the $\text{Au}(001)$ surface. The specular CTR is represented by the thick line labeled $(0\ 0\ L)$. Using the fcc cubic unit cell as a basis, the scattering vector \mathbf{Q} is described in terms of the Miller indices associated with the fcc lattice, (H, K, L) , $H = (a/2\pi)Q_x$, $K = (a/2\pi)Q_y$, and $L = (a/2\pi)Q_z$ where L lies along the surface normal, H and K lie in the plane of the surface, and $a = 4.08$ Å is the lattice constant at room temperature. We also define $a^* = 2\pi/a$ and quote all wave vectors in (H, K, L) units.

Scattering along the specular CTR was measured by integrating the intensity obtained in rocking scans (θ scans) at each point along the rod. This integrated specular reflectivity $R(Q_z)$ was modeled by summing the scattering amplitude from each atomic layer normal to the surface. For the (001) surface of an ideally terminated fcc crystal/vacuum interface the absolute reflectivity is^{13,20,23}

$$R(Q_z) = \frac{I}{I_0} = \left| \frac{2\pi r_o}{a^2} \right|^2 \left| \frac{F(\mathbf{Q})e^{-W}}{2Q_z \sin(Q_z d/2)} \right|^2, \quad (1)$$

where r_o is the electron Thomson radius, $F(\mathbf{Q})$ the atomic form factor, e^{-W} the Debye-Waller factor for the thermal disorder, and d the bulk interlayer spacing ($d = a/2$). For a nonideal surface which is either reconstructed, relaxed, or rough, scattering from the surface layers must be explicitly included. In addition, for a buried interface, absorption and refraction by the liquid overlayer must also be included,¹³

$$R(Q_z) = \left| \frac{2\pi r_o}{a^2} \right|^2 \left| \frac{F(\mathbf{Q})e^{-W}}{Q_z} \right|^2 T^4(Q_z) e^{-Q_{\text{abs}}/Q_z} \times \left| \sum_{m=0}^{\infty} \rho_m e^{-Q_z^2 \sigma_z^2 / 2} e^{iQ_z d(m-\epsilon_m)} \right|^2, \quad (2)$$

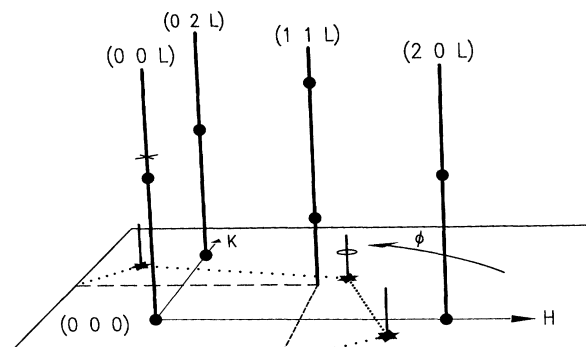


FIG. 2. Schematic diagram of the x-ray scattering from the reconstructed $\text{Au}(001)$ surface in reciprocal space. Filled circles show the positions of Bragg points and the solid lines connecting these points are CTR's. The (measured) specular rod is the $(0\ 0\ L)$. The stars and thinner vertical lines show the positions of the surface rods associated with the reconstruction. Dashed (dotted) lines join the bulk (surface) scattering rods to highlight the square (hexagonal) scattering symmetries.

where $T(Q_z)$ is the Fresnel surface-electric-field-enhancement factor and e^{-Q_{abs}/Q_z} is the absorption of the x rays in the liquid and polypropylene film overlayer (assuming a slab of constant thickness). The electron density of an atomic layer is ρ_m (normalized to a bulk layer), σ_z represents the rms displacements above the Debye-Waller term (due to enhanced thermal motion, static corrugations, and disorder in the surface layers), and ϵ_m is the relative increase in the atomic layer spacing from the bulk value. In practice, at sufficiently large Q_z , $T^4 e^{-Q_{\text{abs}}/Q_z} \approx 1$ and can be ignored. Scattering from the liquid layer itself is diffuse and has been subtraction. Scattering from the top surface of the liquid and the two surfaces of the polypropylene film can be neglected at sufficiently large values of Q_z since the low scattering amplitudes and roughness of these surfaces results in a very fast decrease in scattering intensity with increasing Q_z . Scattering from adsorbed species on the surface can be significant in measurements of the CTR's,²⁴ especially in the presence of high- Z atomic species (e.g., Pb, I). The electrolytes used in this study should contain no significant contamination by such species and scattering from adsorbed species was therefore ignored. Along the specular CTR the longitudinal resolution, $\Delta Q_z = 0.012 \text{ \AA}^{-1}$ half width at half maximum (HWHM), is set by the detector slits. The coherence area for the spectrometer as configured is $\pi^2/(\Delta Q_x \Delta Q_y)$, which is equal to approximately $120 \times 50 \text{ \AA}$ at $L = 2$.

Scattering associated with only the top one or two layers of the crystal can be used to investigate the in-plane structure of the reconstruction. For a hexagonal overlayer on the square bulk surface lattice, this scattering is concentrated into "surface rods" in reciprocal space^{11,14} which have hexagonal symmetry and are extended along the surface normal direction. A representation of these surface rods (which have no contribution from bulk atoms) is shown in Fig. 2 as the short vertical lines arranged in a hexagonal pattern (shown as stars connected by a dotted line). The vertical extent of the surface rods allows the in-plane structure of the monolayer to be investigated at relatively large out-of-plane scattering vectors. This is important since at very small Q_z the x-ray path length in the liquid overlayer is very large and resulting in significant attenuation of the x-ray signal. During this study $L \approx 0.4$ was found to maximize the measured surface rod intensities.

IV. RESULTS

A. Cyclic voltammograms

CV's for the Au(001) crystal in 0.1 M KOH and 0.1 M HClO₄ electrolytes are shown in Figs. 3(a) and 4(a), respectively. These curves were obtained using the hanging meniscus technique. In each case the potential window was opened more positively after each complete cycle. After conducting x-ray experiments, the measurement was repeated using the hanging meniscus technique. These curves were almost identical to the initial curves.

The CV curves for Au(001) in KOH solution [Fig. 3(a)] are very similar to those obtained by Hamelin *et al.*¹⁷ In this case, the currents in the "double-layer" potential region are significant and show a pronounced slant to negative currents at the most negative potentials. This slant of the double-layer region is probably due to the reduction of trace oxygen present in electrolyte. Au(001) has a relatively high catalytic activity for oxygen reduction in alkaline electrolyte¹⁷⁻¹⁹ (orders of magnitude higher than the same surface in HClO₄ solution). The relatively large positive charge transfer in the potential region of -0.25 to 0.0 V in KOH is attributed to adsorption pseudocapacitance from the specific adsorption (with charge transfer) of hydroxyl anions.¹⁸ The adsorption of hydroxyls is a precursor state to the formation of the "true oxide" layer, which begins at 0.25 V. On the negative sweep, reduction of the oxide is essentially completed by -0.25 V, below which the double layer on the negative sweep is relatively featureless.

The current peak just below 0.0 V (and the charge under this peak) was sensitive to the cycling history of the electrode. The dashed curve is the first cycle in which the positive potential limit was above 0.0 V, while the solid curve shows a later potential cycle. Keeping the poten-

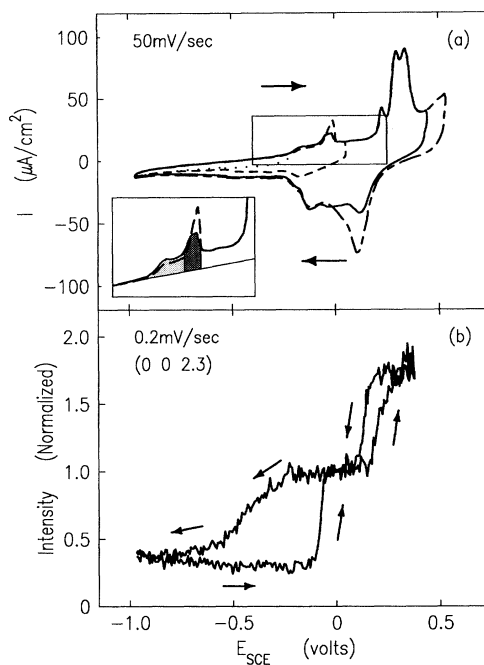


FIG. 3. (a) Cyclic voltammetry in 0.1 M KOH. This curve was measured using the hanging meniscus technique (refer to text). The potential was scanned at 50 mV/sec . The inset shows an expansion of the positive going sweep from approximately -0.4 to 0.25 V. The shaded areas represent the integrated charge associated with hydroxyl adsorption, as described in the text. (b) Scattered intensity at the $(0\ 0\ 2.3)$ position on scanning the potential at 0.2 mV/sec . The scattering intensity was normalized to 1 at the (1×1) interface (near 0.0 V).

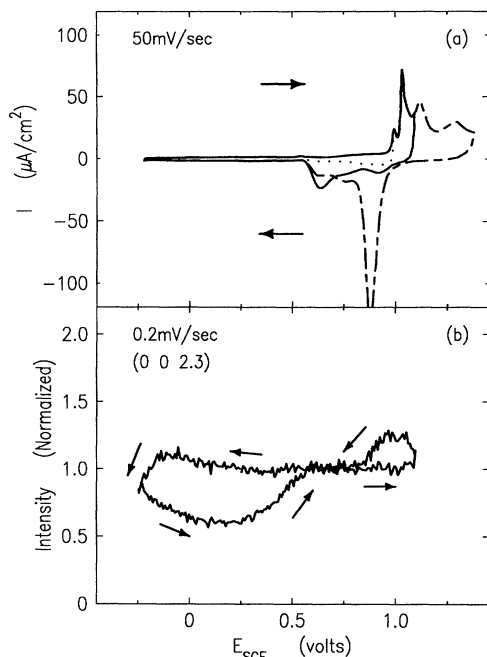


FIG. 4. (a) Cycling voltammetry in 0.1 M HClO_4 . These curves were measured using the hanging meniscus technique (refer to text). The potential was scanned at 50 mV/sec. (b) Scattered intensity at the (0 0 2.3) position on scanning the potential at 0.2 mV/sec. The scattering intensity was normalized to 1 for the (1×1) interface (near 0.7 V).

tial below 0.0 V for a longer period of time *decreases* the charge under the shoulder near -0.20 V, but *increases* the charge under the peak near 0.0 V. This peak appears to be an electrochemical signature of the lifting of the reconstruction (see Sec. IV D) and would coincide to charge from additional adsorption of hydroxyl ions on the unreconstructed surface.

The charge transfer associated with the hydroxyl adsorption was estimated by subtracting the background current due primarily to double-layer charging (estimated by fitting the current between -0.5 and -0.3 V with a straight line and extrapolating to higher potentials) and integrating the charge above this baseline (see Fig. 3, inset). The charge under the solid curve in Fig. 3 (inset) is $29 \mu\text{C}/\text{cm}^2$ for the lightly shaded region (up to -0.07 V) and $27 \mu\text{C}/\text{cm}^2$ for the darkly shaded region (between -0.07 and 0.00 V), corresponding to 15% and 14% of a monolayer, respectively (assuming complete discharge of the anion). For the dashed curve, which was cycled at potentials less than -0.2 V for about two minutes (rather than 35 sec for the prior case), the equivalent charges are $21 \mu\text{C}/\text{cm}^2$ (11% of a monolayer) and $37 \mu\text{C}/\text{cm}^2$ (19% of a monolayer), respectively. The increase in charge under the peak near 0.0 V (from 27 to $37 \mu\text{C}/\text{cm}^2$) is associated with cycling the potential below -0.2 V, and can be interpreted as indicative of the reconstruction forming on a larger fraction of the surface.

The curves in HClO_4 solution [Fig. 4(a)] are essentially

identical to previously published results.^{9,25,26} Cycling positively from 0.8 V, "true oxide" forms, beginning at about 1.0 V. The oxide layer appears to be completely reduced by 0.55 V. The potential region from 0.55 V down to -0.25 V and back to 0.8 V is characterized by very small currents attributed primarily to double-layer charging, and is featureless on this scale.

B. In-plane diffraction

Grazing incidence x-ray-diffraction rocking scans (shown in Fig. 5) were measured to investigate the structure of the Au(001) surface in the plane of the surface. These ϕ scans correspond to scanning through the rods at fixed L along an arc at a fixed distance from the surface (see Fig. 2). The scans shown in Figs. 5(a) and 5(b) for KOH and HClO_4 solutions, respectively, are centered near the (1.2 1.2 0.4) position of the reconstruction surface rod, marked by an "O" in Fig. 2. In both cases the scattering due to the reconstructed surface (shown at -0.67 V for KOH and -0.25 V for HClO_4 solutions) is missing at higher potentials (0.1 and 0.8 V for KOH and HClO_4 electrolytes, respectively). Figure 5(c) is centered at (1 1 0.4), on the $(1 \ 1 \ L)$ bulk rod and shows that the in-plane mosaic spread of the crystal surface has a HWHM of approximately 0.25° . This includes a contribution from the crystal mosaic and the spectrometer resolution.

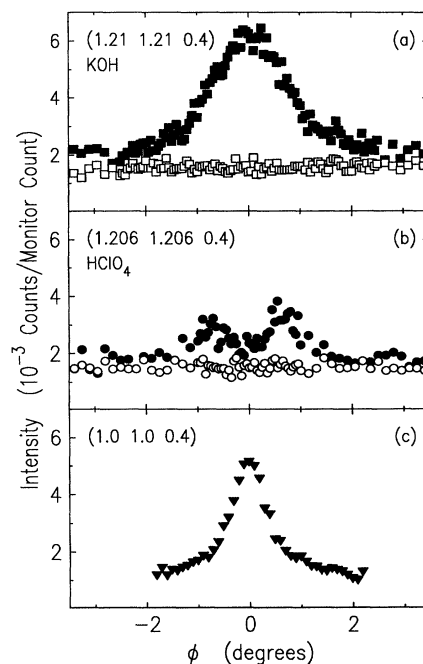


FIG. 5. Glancing-incidence-angle x-ray-diffraction rocking curves of the reconstruction peaks. (a) Peak at (1.210 1.210 0.4) in KOH solution at 0.10 V (open) and -0.67 V (filled). (b) Peak at (1.206 1.206 0.4) in HClO_4 solution at 0.80 V (open) and -0.25 V (filled). (c) Rocking curve at the (1 1 0.4) bulk rod position for comparison.

The Au(001) in KOH electrolyte gave rise to only one broad peak, aligned along the [110] direction [Fig. 5(a)], indicative of a hexagonal reconstruction. This peak is located at (1.210 1.210), uncertainty ± 0.005 , consistent with an incommensurate reconstruction. The domain size was estimated from the reciprocal of the HWHM convoluted with the domain width [estimated from the peak width at (1 1 0.4)]. From this procedure the calculated domain size was only approximately 40 Å in the direction perpendicular to the [110] axis.

In HClO₄ solution at -0.25 V [Fig. 5(b)], the two peaks centered at (1.206 1.206), uncertainty ± 0.005 , are due to an incommensurate-hexagonal reconstruction, rotation $\pm 0.7^\circ$ from the [110] direction (a rotation of $\pm 0.55^\circ$ was measured after only a few potential cycles). Apart from being somewhat broader and weaker, the reconstruction peaks are similar to the peaks previously measured for Au(001)/vacuum interface.¹⁴ The calculated domain size was approximately 100 Å in the direction perpendicular to the [110] axis, considerably larger than found in KOH solution. The results in HClO₄ solution differ in no significant respect from previous results.¹¹ While it is difficult to directly compare the in-plane intensities between two different systems (due to liquid absorption and beam footprint variations, etc.), the similarity of the background scattering and the considerable differences in the surface rod intensity suggest that the fraction of the surface giving rise to this peak is much greater in KOH than in HClO₄ solution.

C. Specular reflectivity measurements

Figure 6 shows the (0 0 *L*) rod measured in KOH solution at -0.67 V (filled squares) and 0.10 V (open squares, $\times 0.01$). Similarly, Fig. 7 shows the same scans in HClO₄ solution at -0.25 V (filled circles) and 0.80 V (open circles, $\times 0.01$). In the figures a dashed line shows the scattering which would be expected from an ideal interface, i.e., sharp termination of the (1 \times 1) lattice [see Eq. (1)]. For the rods measured at the higher potentials, the scattering between the Bragg peaks lies below the ideal value for all *L*, suggesting that the surface is more diffuse ("rougher") than the ideal surface. At the lower potentials in both electrolytes, the rods show a pronounced asymmetry, with enhanced reflectivity just below the (0 0 2) position and reduced reflectivity above the (0 0 2) position. This is indicative of a top layer which is displaced outwards from the expected bulk surface position, as is the case for the vacuum reconstruction.¹³

The CTR data were modeled using the form described in Eq. (2) for scattering vectors greater than $L = 0.3$. The (1 \times 1) surfaces (Figs. 6 and 7, bottom) were modeled using two methods: allowing the surface disorder term to vary and fixing the surface occupation at unity, or allowing fractional occupation of the top atomic layer and using the vacuum surface rms displacement terms. The results given in Table I show that the Au(001) surface in both electrolytes are very similar and well represented by either an enhanced disorder of the top layer or a partial occupation (15–25%) of the top layer (the qual-

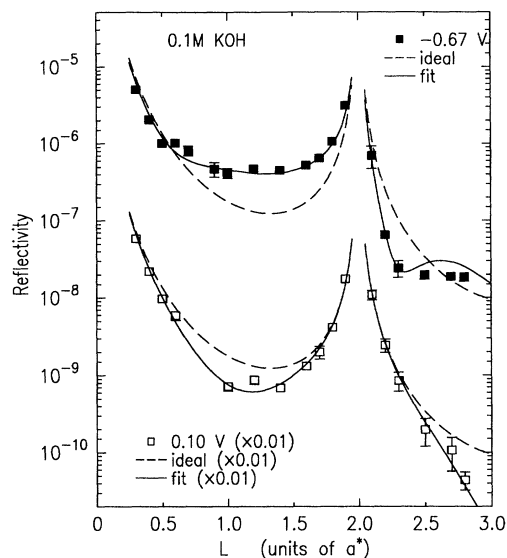


FIG. 6. Absolute reflectivity scans of the (0 0 *L*) rod at -0.67 V (solid squares) and 0.10 V (open squares, $\times 0.01$) in 0.1 M KOH solution. The dashed lines are the ideal reflectivity. The solid lines are fits described in the text with the parameters given in Table I.

ity of our data does not allow us to distinguish between these two models). The solid lines in Fig. 6 (bottom) and Fig. 7 (bottom) show models representing structures with reduced top-layer occupation and vacuum surface disorder (Table I, last line for each system).

The reconstructed surfaces in the two electrolytes

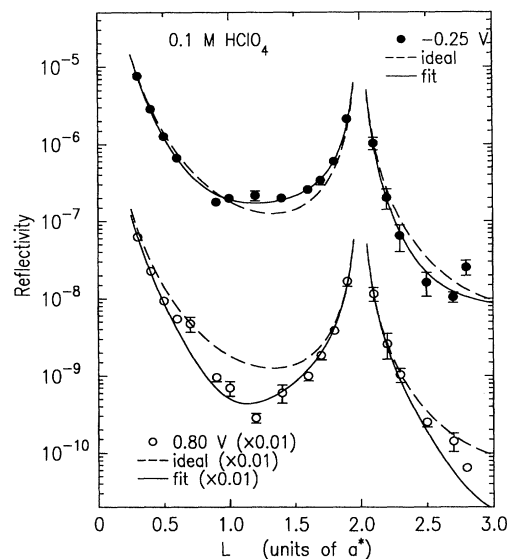


FIG. 7. Absolute reflectivity scans of the (0 0 *L*) rod at -0.25 V (solid circles) and 0.80 V (open circles, $\times 0.01$) in 0.1 M HClO₄ solution. The dashed lines are the ideal reflectivity. The solid lines are fits described in the text with the parameters given in Table I.

[Fig. 6 (top) and Fig. 7 (top)], while qualitatively similar, are not identical. In KOH solution [Fig. 6 (top)], the data are well represented by a model which uses essentially the same parameters used to model the vacuum surface, with only overall intensity and electrolyte film thickness varied (attempts to fit these parameters did not significantly improve the fit quality).

For the reconstructed surface in HClO₄ solution [Fig. 7 (top)], reflection intensity near the (001) anti-Bragg point is significantly lower than in the KOH solution and slightly lower than previously determined in 0.01 M HClO₄ solution.¹¹ While unambiguous determination of the surface structure proved elusive, conclusions on the likely structure can still be made through fitting. Three descriptions of the surface structure were attempted, each using the top-layer density and expansion determined for the vacuum surface¹³ (Table I). A model which featured a partially reconstructed surface with the vacuum determined top-layer rms displacement parameter was found to give relatively poor fits ($\chi^2 = 9.0$) and was therefore discounted. A second model which represented a fully reconstructed surface with increased top layer rms displacements gave good fits ($\chi^2 = 1.9$), but the rms displacements necessary were significantly larger than previously determined.¹¹ The third model, which represented a partially reconstructed surface with increased top-layer rms displacements, gave the best fit ($\chi^2 = 1.5$), and had rms surface displacements consistent with previous study,¹¹ provided approximately 50% of the surface remained unreconstructed [solid line, Fig. 7 (top)]. Gao, Hamelin, and Weaver⁹ found in a STM study that at similar potentials a significant fraction of the surface was unreconstructed. The difference between our results and Ref. 11 might be a function of the more negative potentials used previously (-0.5 V compared to -0.25 V in this study), perhaps allowing a greater fraction of the surface to reconstruct.

To summarize, at sufficiently negative potentials the Au(001) surface is reconstructed in both KOH and HClO₄ electrolytes. In KOH electrolyte the surface normal rms displacements are consistent with those found in

UHV. In contrast, the rms displacements are significantly larger in HClO₄ solution, and, in our study, it appears that the surface is not completely reconstructed. At more positive potentials the reflectivity can be described by a (1×1) model in both electrolytes.

D. Kinetic studies

Figures 3(b) and 4(b) show the intensity [normalized to 1.0 for the (1×1) surface] at the $(0\ 0\ 2.3)$ position on cycling the potential at 0.2 mV/sec in the KOH and HClO₄ solutions, respectively [the location of this point in reciprocal space is marked by an "X" on the $(0\ 0\ L)$ rod of Fig. 2]. These figures are shown with the CV curves for comparison (although the ratio of scan rates of approximately 250:1 should be noted). The purpose of these data are to show the potentials at which changes to the surface structure occur. From the reflectivity analysis in Sec. IV C, the formation of the reconstruction results in a *reduction* of scattering at the $(0\ 0\ 2.3)$ position.

In KOH solution, starting at 0.0 V [(1×1) surface] and sweeping negatively, the reconstruction begins to form at about -0.25 V, with the surface essentially completely reconstructed by -0.60 V. Further sweeping to 0.03 V and back to -0.10 V results in little further change in surface structure. The reconstruction is rapidly lifted in a potential range of approximately 40 mV beginning at -0.10 V. Sweeping positive of 0.15 V results in a rapid structural change, presumably due to the formation of a "place exchanged" surface oxide, AuOH. After sweeping the potential up to 0.37 V, this oxide is fully reduced by 0.10 V. Essentially the same shape as shown in Fig. 3 was obtained with scan rates up to 10 mV/sec (the maximum rate with reliable statistics).

For the HClO₄ solution, the direction of the scattering intensity changes with potential are the same as those found in the KOH solution. The rates and the potentials at which these changes occur are, however, quite different, as is the overall shape of the curve and the smaller variations of the scattered intensity with potential. Again

TABLE I. The top-layer density ρ_0 , surface layer expansion ϵ , and the rms surface displacement amplitudes, σ , for fits to the $(00L)$ rods ($\sigma = 0.085$ Å for bulk atoms). In addition, f is the fraction of surface which was *not* reconstructed (see text). For each electrolyte and potential, the bottom line of parameters is that used to create the line shown in Figs. 7 and 6. The asterisk denotes parameters that were kept fixed.

Electrolyte	Potential V _{SCE}	χ^2	ρ_0	ϵ_0	σ_0 (Å)	σ_1 (Å)	f
KOH	-0.67	2.8	1.26*	0.20*	0.30*	0.16*	0.0*
KOH	0.10	2.8	1.0*	0.0*	0.42	0.16*	1.0*
KOH	0.10	0.9	0.16	0.0*	0.30*	0.16*	1.0*
HClO ₄	-0.25	9.0	1.26*	0.20*	0.30*	0.16*	0.69
HClO ₄	-0.25	1.9	1.26*	0.20*	0.61	0.14	0.0*
HClO ₄	-0.25	1.5	1.26*	0.20*	0.47	0.09*	0.46
HClO ₄	0.80	1.7	1.0*	0.0*	0.52	0.16*	1.0*
HClO ₄	0.80	3.9	0.23	0.0*	0.30*	0.16*	1.0*

beginning with the unreconstructed surface near 0.7 V, the intensity rises slightly on decreasing the potential until -0.15 V where the reconstruction begins to form. On reversing the potential sweep at -0.25 V, the reconstruction continues to form until about 0.20 V. In fact, cycling the potential between -0.25 and 0.25 V results in increased formation of the reconstruction.¹¹ Above approximately 0.25 V the reconstruction begins to lift, with the (1×1) surface fully restored by 0.55 V. Further changes do not take place until 1.10 V, where the onset of oxide formation occurs. The structural changes associated with the oxide are reversed by approximately 0.85 V. A brief description of some observations made in the oxide formation region are presented in the Appendix. The slower kinetics of reconstruction formation in HClO_4 solution resulted in the observation of no changes to the scattering at scan rates of 10 mV/sec.

Another set of measurements of the kinetics of structural change consisted of measuring the scattering at the $(0\ 0\ 2.3)$ position while the potential was stepped between two different values. Representative results from these measurements are shown in Fig. 8. In KOH solution the reconstruction formed in a much wider potential window. Figure 8(a) shows the effect of stepping first from -0.97 to 0.08 V ($T \approx -250$ sec). Within the resolution of our measurements (each point took 20 sec to count) the lifting of the reconstruction was instantaneous. The step to -0.70 V ($T \approx 0$ sec, solid line) was best modeled using two time constants. The fast change has an exponential time constant of approximately 15 sec, and the slow change a time constant of 150 sec, with the fast change accounting for approximately 60% of the intensity decrease. These values are typical for potential steps from near 0.10 V to less than -0.20 V. Steps to -0.20 V resulted in a less reconstructed surface (approximately 60%), while steps to -0.15 V resulted in no reconstruction (dashed line).

The potential stepping measurements in HClO_4 solution were measured after the sample had been exposed to the x-ray beam for approximately 18 hours. Figure 8(d) shows the effect of stepping the potential from -0.3 to 0.80 V at time $T \approx -200$ sec (solid line). As was found in KOH solution, the reconstruction was immediately lifted on stepping the potential to 0.80 V. On stepping the potential to -0.15 V (solid line), the reconstruction formed slowly, with a typical time constant of about 140 sec. Similar behavior was found for steps from 0.80 V to potentials less than approximately 0.0 V. On stepping from 0.80 V to potentials above 0.0 V (a potential step to 0.05 V is shown with a dashed line) the scattering was unchanged or increased slightly. Surprisingly, holding the potential at 0.10 V for a few minutes before stepping to -0.15 V resulted in a much longer time constant (≈ 1000 sec) than stepping from 0.8 V.

The above results led us to suspect that specific adsorption of impurity anions was playing a role in the formation and lifting of the reconstruction in our HClO_4 electrolyte. To investigate the influence of chloride contamination,²⁷ a small amount of HCl was added to the HClO_4 solution (the precise amount was unknown, but is estimated to be 10–100 ppm, or approximately

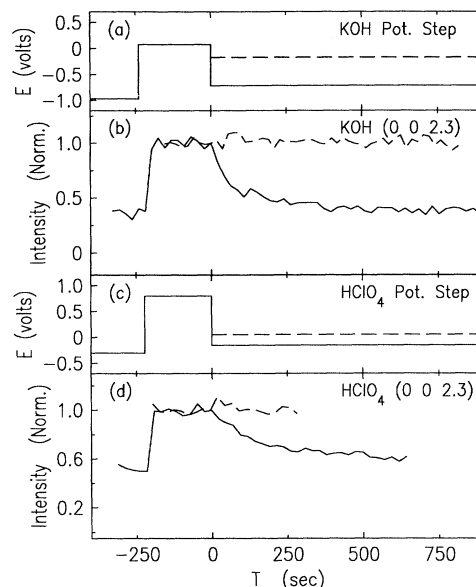


FIG. 8. Effect of stepping the potential on the scattering intensity at the $(0\ 0\ 2.3)$ position. Potential step (a) and scattering intensity (b) for KOH solution. Potential step (c) and scattering intensity (d) for HClO_4 solution. In each case the solid lines show a typical step to a potential at which the reconstruction forms and the dashed lines show the effect of stepping to the lowest potential at which the reconstruction did not form. The count rate for the (1×1) surface has been normalized to 1.

5×10^{-6} – 5×10^{-5} M in chloride) and further potential stepping and cycling studies performed. Stepping studies showed a similar behavior to that in “clean” HClO_4 solution, except that the potential for reconstruction formation was now below -0.1 V, rather than below 0.0 V, and holding the potential near 0.3 V now had the effect of inhibiting formation of the reconstruction. Furthermore, cycling the potential at 1 mV/sec and measuring the scattering at the $(0\ 0\ 2.3)$ position gave no evidence of reconstruction. These results indicate that chloride ions, even when present in very low concentrations, can inhibit the formation of the reconstruction. Indeed, further addition of approximately 10^{-3} M HCl resulted in complete inhibition of the reconstruction above -0.3 V.

V. DISCUSSION

This study has shown that the Au(001) surface in contact with KOH electrolyte is reconstructed at sufficiently negative potentials, and reconfirmed the formation of the reconstruction in HClO_4 electrolyte. In both electrolytes the principal features of the reconstruction are consistent with the features of the vacuum interface. In KOH electrolyte, some differences are that the surface reconstruction domains are much smaller than the domains found in HClO_4 solution or in vacuum, and the reconstructed hexagonal overlayer is oriented along the $[110]$ direction (and not rotated from it, as is the case in vacuum).

In HClO_4 solution, our results confirm previous studies,^{9,11} although the smaller potential region we used here seems to have precluded complete reconstruction of the surface. The reconstruction consists of a hexagonal overlayers rotated slightly away from the [110] direction, although specular reflectivity indicates that the top layer has a larger disorder or buckling of the top layer than was found in vacuum or KOH solution.

Besides the slightly different structures of the reconstruction of Au(001) in KOH and HClO_4 electrolytes, there are significant differences in the kinetics and in the potential regions for the structural transitions. The potentials at which the reconstruction forms and the regions over which it is stable are summarized in Fig. 9. This and Figs. 3 and 4 show that the hysteresis of reconstruction formation and lifting in alkaline electrolyte is much smaller than in HClO_4 solution. In addition, the reconstruction forms much more rapidly in KOH solution than in HClO_4 solution (of order 15 and 100 sec, respectively).

Following the discussion of the thermodynamic driving force for the potential-dependent reconstruction of Au(001)/electrolyte interface presented by Ross and D'Agostino,²⁸ we note that theoretically *in the absence of adsorption* the reconstructed surface is expected to be thermodynamically favored over the unreconstructed surface at all potentials. Theoretical calculations have shown that the difference in surface energy, γ , between the clean vacuum reconstructed and unreconstructed surfaces^{15,16} is approximately 0.1 eV/atom, which, while large compared to the change in surface energy due to potential charging in the double layer, is smaller than the energy gained by adsorption of anions (e.g., hydroxyl or chloride), which can lower the surface energy by 1–5

eV/atom. This suggests that electrolyte containing anions which interact strongly with the surface could cause the reconstruction to form (lift) in the potential range where anion desorption (adsorption) occurs, generally in the potential region near the potential of zero charge [PZC (Ref. 29)]. Since the PZC for the reconstructed surface (PZC^{R}) is 0.15–0.20 V *more positive* than the PZC of the unreconstructed surface (PZC^{U}), anions will generally adsorb on the unreconstructed surface at potentials lower than they will adsorb on the reconstructed surface. This suggests that in an electrolyte containing a strongly interacting anion, the reconstruction will lift at a potential slightly higher than PZC^{U} , whereas if the anions present are only weakly interacting then the reconstruction will be stable up to much higher potentials, well positive of PZC^{U} (see Fig. 11 of Ref. 28).

The PZC's for Au(001) in KOH electrolyte have not been measured. However, we estimate that in 0.1 M KOH solution $\text{PZC}^{\text{R}} \approx 0.0 \pm 0.1$ V and $\text{PZC}^{\text{U}} \approx (\text{PZC}^{\text{R}} - 0.17) \pm 0.05$ V (approximately -0.17 V).³⁰ These and the PZCs determined in 0.01 M HClO_4 solution²⁸ are shown with arrows in Fig. 9. The values in KOH solution are slightly negative of the measured values in HClO_4 solution due to the adsorption of hydroxyl anions.³¹ The capacitance shown in Fig. 3 in this potential region, which is associated with the electroadsorption of hydroxyl anions, is consistent with these estimates of PZC^{R} and PZC^{U} . With these assumptions, the reconstruction in KOH does indeed appear to be stable up to a potential positive of PZC^{U} . The relative changes in surface energy due to hydroxyl ion adsorption appears to be the thermodynamic driving force for these reversible transitions in surface structure in KOH solution. The thermodynamic description alone, however, predicts that the reconstruction transition is completely reversible, and this is clearly not the case in either electrolyte. Therefore, kinetic effects must be included in the description of the transformation. In the potential range between PZC^{U} and PZC^{R} the surface coverage with hydroxyl anions on the reconstructed surface (positive potential sweep) is much lower than the surface coverage on the unreconstructed surface (negative potential sweep). The hysteresis in this case can, therefore, be understood provided the hydroxyl anions "pin" the unreconstructed surface in a metastable state (probably by limiting Au atom mobility) and thereby inhibit surface reconstruction. The reconstruction only begins to form when the hydroxyl anions are substantially desorbed from the surface, an event which should occur at or just below PZC^{U} . This seems reasonable since the hysteresis between the lifting of the reconstruction and the beginning of reconstruction formation is approximately the expected potential separation between the two PZC's.³²

The situation in HClO_4 solution seems more unclear. Electrochemical studies have shown that perchlorate anions interact with the Au(001) surface less than hydroxyl anions,²⁶ in which case the reconstruction should lift at potentials well positive of PZC^{U} . The results in Figs. 4 and 9 show that the reconstruction lifts over a broad range of potentials just above PZC^{R} and, in contrast to the results in KOH electrolyte, the reconstruction re-

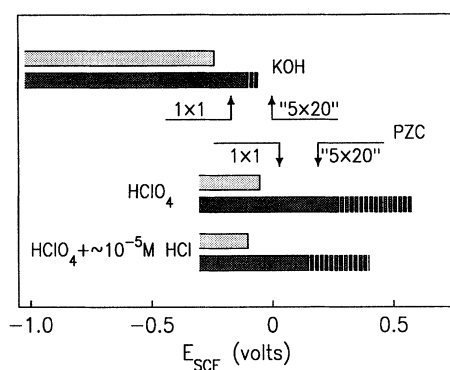


FIG. 9. Summary of the potentials at which the Au(001) surface will initially reconstruct and, once formed, the region of stability. The initial formation was obtained from stepping the potential from approximately 0.1 V (KOH solution) and 0.8 V (HClO_4 solution). The stability was determined from slowly sweeping the potential at 1 mV/sec or less. The broken bars show the region over which the reconstruction lifted, as determined from the scattering intensity at the (0 0 2.3) position. The arrows show the approximate locations of the estimated PZC's for the different surfaces in the two principal electrolytes (refer to text). The bars are shown down to the potential for hydrogen evolution.

forms slowly at potentials much less than PZC^U . This latter observation is difficult to reconcile with the theoretical treatment outlined above unless another anion is controlling the reconstruction transformation. This is conceivable since commercially available $HClO_4$ solution is known to be contaminated with chloride anions²⁷ and we observed that the addition of trace quantities (10–100 ppm) of chloride anions to $HClO_4$ electrolyte caused a significant negative shift in the potential for formation of the reconstruction. In addition, exposure of the $HClO_4$ electrolyte to the x rays may have resulted in the decomposition of the perchlorate anion, releasing an additional small quantity of chloride into solution. Together these observations suggest that *specific* adsorption of an impurity chloride anions may play an important role in the kinetics of the Au(001) surface in $HClO_4$ solution. Due to the low concentrations of chloride in our electrolyte, however, the maximum coverage in our experiments should be quite low (of order 0.1 monolayers or less). This suggests that chloride anions play a significant role only on the kinetics of the reconstruction (i.e., the coverage is too low to have a significant effect on γ). At very low coverages, chloride is expected to be adsorbed preferentially at steplike defects,³³ which might inhibit formation of the reconstruction since Au atoms from step edges are the most probable source of additional atoms needed to form the denser reconstructed layer.⁹ Diffusion of chloride anions (from the thin layer cell and bulk) control the lifting of the reconstruction, resulting in the slow kinetics just above PZC^R [well above this potential (near 0.7 V) significant hydroxyl (or perhaps perchlorate) anion adsorption might be responsible for the much more rapid lifting]. The formation of the reconstruction would also be controlled by chloride anion desorption from the unreconstructed surface. The observations of an inhibition of formation of the reconstruction at low potential by a prior holding of the potential in a region where chloride would be expected to adsorb (0.3–0.7 V) with an explanation involving diffusion of the anion. The rapid lifting of the reconstruction on stepping the potential to 0.8 V suggests that the lifting mechanism may be a function of the potential. While these explanations of possible effects of a chloride impurity in the $HClO_4$ may be plausible, they are still speculations. Definitive results for $HClO_4$ solution await studies in specially purified “chloride-free” electrolyte.

The slightly different reconstructed surface structures observed in KOH and $HClO_4$ solutions may be a consequence of the anions present on the surface during the initial reconstruction. In KOH solution the reconstruction forms on a surface which has some hydroxyl anions adsorbed, whereas in $HClO_4$ solution the (001) facets are devoid of adsorbed anions. Alternatively, the difference structures could be a consequence of the very different rates at which the reconstruction forms. Previous results in $HClO_4$ solution have lead some authors to propose that a negative charge on the Au(001) surface from double-layer electric-field charging is needed to form the reconstruction in solution.^{7,9} While our results in KOH solution do not provide any conclusive results on this question, they do indicate that for this model

to be correct the required charge must be much smaller than previously proposed. Our results also suggest that anion/surface interactions alone may be sufficient to explain the observed behavior.³⁴ A surprising aspect of the Au(001) reconstruction phase transition in electrolyte is that it occurs at all at room temperatures.⁷ The fact that it occurs very rapidly indicates that the energetics must be quite different for the surface in solution versus the same surface in vacuum.

VI. SUMMARY

In this study we have used x-ray diffraction to investigate the reconstruction of the Au(001) interface with KOH and $HClO_4$ solutions. In both cases the surface reconstructs at sufficiently negative potentials, the reconstructions consisting of incommensurate-hexagonal overlayers which are similar, but not identical, to the reconstruction found at the vacuum interface. In both electrolytes the reconstructed surface appears to be stable to potentials close to PZC^R . In KOH, formation of the reconstruction begins only about 150 mV negative of the lifting potential, a potential separation approximately equal to the separation of the work functions or PZC 's for the reconstructed and unreconstructed surfaces. In $HClO_4$, the separation in potential is much greater, with lifting of the reconstruction at about 0.1 V above PZC^R . The reduced potential region of stability of the reconstruction in KOH appears to be due to adsorption of hydroxyl anions near PZC^R . Comparing the reconstruction in KOH and $HClO_4$ solutions, in the former the surface reconstructs much more rapidly into smaller domains, is more ordered along the surface normal direction, and in-plane is aligned exactly along the [110] direction. The fast kinetics in KOH electrolyte indicate that the energy barrier for the unreconstructed to reconstructed surface transition must be significantly lower than the energy barrier for the vacuum interface. In contrast, the reconstruction in $HClO_4$ solution is much slower, and requires several minutes. The mechanism for the formation and lifting of the reconstruction in $HClO_4$ is unclear, although trace quantities of a specifically adsorbing anion (such as chloride) may play a significant role.

ACKNOWLEDGMENTS

We would like to thank Lee Johnson for technical assistance and acknowledge very useful discussions with Ben Ocko, Jia Wang, and Michael Toney. This work was supported by the Director, Office of Energy Research, Office of Basic Energy Science, Materials Sciences Division of the U.S. Department of Energy under Contract No. DE-AC03-76SF00098. Research carried out in part at the NSLS, Brookhaven National Laboratory, which is supported by the U.S. Department of Energy, Division of Materials Sciences and Division of Chemical Sciences (DOE Contract No. DE-AC02-76CH00016). X16-B is supported by AT&T Bell Laboratories.

APPENDIX: GOLD OXIDE

Although the formation of the gold oxide is an interesting and complex problem which was not the primary subject of this study, a few observations can be made at this time. From the CV curves shown in Figs. 3 and 4 it appears that for both electrolytes the oxide forms approximately 1.25 V positive of the potential for hydrogen evolution. In both cases, oxide formation and reduction are complex, multistep, sweep-rate-dependent processes. In KOH solution, the current peaks prior to oxygen evolution are relatively broad, whereas in HClO₄ solution they are much sharper, which suggests that in this case oxide formation is concurrent with anion desorption.²⁶ The significance of the multiple current peaks is unknown. The x-ray scattering results reveal that in KOH solution the oxide formation appears to be a single structural step process which occurs near 0.15 V. A similar structural change is observed in HClO₄ solution, although the change does not occur until approximately 1.1 V and shows considerably more hysteresis upon reduction. It is interesting to note that this structural change occurs after approximately the same charge has passed in both electrolytes (about 52 and 61 $\mu\text{C}/\text{cm}^2$ for KOH

and HClO₄ solutions, respectively). The greater hysteresis in HClO₄ solution is possibly due to incorporation of anions into the oxide layer which stabilize the surface. What is perhaps most surprising is the direction of the change to the scattering. The *increase* in scattering suggests that there is a contraction of the distance between the top ordered layer and the next layer. An attempt was made to measure the (0 0 L) truncation rod in KOH electrolyte solution at a potential of 0.35 V. Although the surface structure was found to be somewhat unstable while held for the two hours necessary to measure the reflectivity, it nevertheless showed that the scattering was increased above $L = 2$ but significantly decreased near $L = 1$. While we were unable to obtain a satisfactory fit, the general shape of the reflectivity seems to indicate the existence of a wide, rough interface, in which the top commensurate gold layer is compressed. We speculate that this may result when "place exchange" occurs between the top layer of gold atoms and an oxygenated species (hydroxyl?) adsorbed at the interface. If this top structure is disordered, it would lead to a broad interfacial width [decreasing the scattering around (0 0 1)] and a compression of the top commensurate layer of gold. While this result is intriguing, further more detailed studies are needed to determine the surface morphology.

* Permanent address: Institut of Electrochemistry, ICTM, University of Belgrade, Belgrade, Yugoslavia.

¹ D. G. Fedak and N. A. Gjostein, *Surf. Sci.* **8**, 77 (1967).

² M. A. Van Hove, R. J. Koestner, P. C. Stair, J. P. Bibérian, L. L. Kesmodel, I. Bartös, and G. A. Somorjai, *Surf. Sci.* **103**, 189 (1981); **103**, 218, (1981).

³ A. Hamelin, *J. Electroanal. Chem.* **142**, 299 (1982).

⁴ E. Yeager, W. E. O'Grady, M. Y. C. Woo, and P. Hagans, *J. Electrochem. Soc.* **125**, 346 (1978).

⁵ D. M. Kolb, G. Lehmpfuhl, and M. S. Zei, *J. Electroanal. Chem.* **179**, 289 (1984).

⁶ All potentials in this paper are referenced to the saturated calomel electrode (SCE). The SCE reference is used since it is independent of pH.

⁷ D. M. Kolb, *Ber. Bunsenges. Phys. Chem.* **92**, 1175 (1988); in *Structure of Electrified Interfaces*, edited by P. N. Ross and J. Lipkowski (VCH, New York, 1993).

⁸ O. M. Magnussen, J. Hotlos, R. J. Nichols, D. M. Kolb, and R. J. Behm, *Phys. Rev. Lett.* **64**, 2929 (1990); R. J. Nichols, O. M. Magnussen, J. Hotlos, T. Twomey, R. J. Behm, and D. M. Kolb, *J. Electroanal. Chem.* **290**, 21 (1990).

⁹ X. Gao, A. Hamelin, and M. J. Weaver, *Phys. Rev. Lett.* **67**, 618 (1991); *Phys. Rev. B* **46**, 7096 (1992).

¹⁰ M. G. Samant, M. F. Toney, G. L. Borges, L. Blum, and O. R. Melroy, *J. Phys. Chem.* **92**, 220 (1988); O. R. Melroy, M. F. Toney, G. L. Borges, M. G. Samant, J. B. Kortright, P. N. Ross, and L. Blum, *Phys. Rev. B* **38**, 10962 (1988).

¹¹ B. M. Ocko, J. Wang, A. Davenport, and H. Isaacs, *Phys. Rev. Lett.* **65**, 1466 (1990); B. M. Ocko and J. Wang, in *Structural Effects in Electrocatalysis and Oxygen Electrochemistry*, edited by D. Scherson, D. Tryk, M. Daroux,

and X. Xing (The Electrochemical Society, Pennington, NJ, 1992).

¹² G. Binnig, H. Rohrer, Ch. Gerber, and E. Stoll, *Surf. Sci.* **144**, 321 (1984).

¹³ B. M. Ocko, D. Gibbs, K. G. Huang, D. M. Zehner, and S. G. J. Mochrie, *Phys. Rev. B* **44**, 6429 (1991).

¹⁴ D. Gibbs, B. M. Ocko, D. M. Zehner, and S. G. J. Mochrie, *Phys. Rev. B* **42**, 7330 (1990); D. L. Abernathy, S. G. J. Mochrie, D. M. Zehner, G. Grubel, and D. Gibbs, *ibid.* **45**, 9272 (1992).

¹⁵ F. Ercolessi, E. Tosatti, and M. Parrinello, *Phys. Rev. Lett.* **57**, 719 (1986); F. Ercolessi, A. Bartolini, M. Garofalo, M. Parrinello, and E. Tosatti, *Surf. Sci.* **189/190**, 636 (1987).

¹⁶ N. Takeuchi, C. T. Chan, and K. M. Ho, *Phys. Rev. Lett.* **63**, 1273 (1989); *Phys. Rev. B* **43**, 14363 (1991).

¹⁷ A. Hamelin, M. J. Sottomayor, F. Silva, S.-C. Chang, and M. J. Weaver, *J. Electroanal. Chem.* **295**, 291 (1990).

¹⁸ R. Adžić, N. M. Marković, and V. B. Vesović, *J. Electroanal. Chem.* **165**, 105 (1984).

¹⁹ J. D. E. McIntyre and W. F. Peck, in *The Chemistry and Physics of Electrocatalysis*, edited by J. D. E. McIntyre, M. J. Weaver, and E. B. Yeager (The Electrochemistry Society, Princeton, NJ, 1984); R. Adžić, *Adv. Electrochem. Electrochem. Eng.* **13**, 163 (1984).

²⁰ R. Feidenhans'l, *Surf. Sci. Rep.* **10**, 105 (1989); E. Vlieg, J. F. van der Veen, S. J. Gurman, C. Norris, and J. E. Macdonald, *Surf. Sci.* **210**, 301 (1989); I. K. Robinson, in *Handbook of Synchrotron Radiation*, edited by D. E. Moncton and G. S. Brown (North-Holland, Amsterdam, 1991), Vol. 3; I. K. Robinson and D. J. Tweet, *Rep. Prog. Phys.* **55**, 599 (1992).

- ²¹ N. Marković, M. Hanson, G. McDougal, and E. Yeager, *J. Electroanal. Chem.* **214**, 555 (1986).
- ²² A. Hamelin, X. Gao, and M. J. Weaver, *J. Electroanal. Chem.* **323**, 361 (1992).
- ²³ I. K. Robinson, *Phys. Rev. B* **33**, 3830 (1986).
- ²⁴ J. Wang, B. M. Ocko, A. Davenport, and H. Isaacs, *Phys. Rev. B* **46**, 10321 (1992).
- ²⁵ F. Silva, M. J. Sottomayor, A. Hamelin, and L. Stoicoviciu, *J. Electroanal. Chem.* **295**, 301 (1990).
- ²⁶ H. Angerstein-Kozłowska, B. E. Conway, A. Hamelin, and L. Stoicoviciu, *Electrochim. Acta* **31**, 1051 (1986).
- ²⁷ B. D. Cahan, H. M. Villullas, and E. B. Yeager, *J. Electroanal. Chem.* **306**, 213 (1991).
- ²⁸ P. N. Ross and A. T. D'Agostino, *Electrochim. Acta* **37**, 615 (1992).
- ²⁹ The PZC is the potential at which an ideally polarizable surface emersed in an electrolyte will have a net zero charge at the interface. The PZC is closely related to the work function for the vacuum interface. Ross and D'Agostino (Ref. 28) reported values in 0.01 M HClO₄ solution of 0.19 and 0.04 V for the reconstructed and unreconstructed surfaces, respectively. Kolb and Schneider [*Electrochim. Acta* **31**, 929 (1986)] reported values of 0.30 and 0.08 V for the same surfaces. These differences are probably due to differences in the detailed surface structure (Ref. 33) and do not affect our conclusions.
- ³⁰ These estimates were obtained by relating PZC^R and PZC^U to the PZC of polycrystalline Au (PZC^{POLY}) in both acid and alkaline electrolyte. The relative potentials of PZC^R, PZC^U, and PZC^{POLY} for an ideal metal should be independent of the pH [S. Trasatti, in *Modern Aspects of Electrochemistry*, edited by B. E. Conway and J. O'M. Bockris (Plenum, New York, 1979), Vol. 13]. Using this information we estimate PZC^R and PZC^U in 0.1 M KOH electrolyte by using the known values determined in HClO₄ electrolyte (e.g., PZC^R ≈ PZC^{POLY} + 0.3 V) and scaling to the value of PZC^{POLY} in 0.1 M NaOH electrolyte, which is estimated (Ref. 31) to be -0.3 V.
- ³¹ D. D. Bodé, T. N. Andersen, and H. Eyring, *J. Phys. Chem.* **71**, 792 (1967); T. N. Andersen, J. L. Anderson, and H. Eyring, *ibid.* **73**, 3562 (1969).
- ³² The Au(001) surface in 0.01 M KBr electrolyte (Ref. 11) was found to have a slightly greater hysteresis between the lifting and formation of the reconstruction (about 0.05 V). The larger hysteresis can be understood since bromide anions are believed to be chemisorbed (rather than electrosorbed as are hydroxyl anions) and as such require a more negative potential to desorb.
- ³³ P. N. Ross, *J. Chim. Phys.* **88**, 1353 (1991).
- ³⁴ It has been noted that the lifting and formation of the Au(111) surface reconstruction in 0.1 M NaF, NaCl, and NaBr electrolytes seems to coincide with *anion adsorption* corresponding to an induced surface charge density of 0.07 electrons per atom [see Ref. 24 and J. Wang, B. M. Ocko, A. Davenport, and H. Isaacs, *Science* **255**, 1416 (1992)].